MRC Technical Summary Report #1714
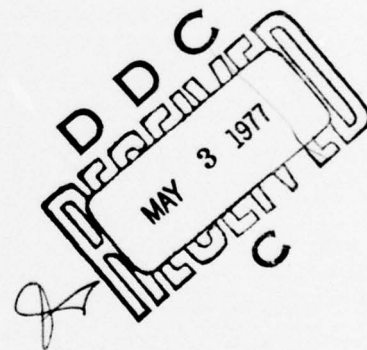
SOME GLOBAL EQUILIBRIUM SURFACES

M. J. Sewell

See 1473

Mathematics Research Center
University of Wisconsin—Madison
610 Walnut Street
Madison, Wisconsin 53706

February 1977

(Received November 23, 1976)

DDC
MAY 3 1977

Approved for public release
Distribution unlimited

UNIVERSITY OF WISCONSIN - MADISON
MATHEMATICS RESEARCH CENTER

SOME GLOBAL EQUILIBRIUM SURFACES

M. J. Sewell

Technical Summary Report #1714

February 1977

ABSTRACT

Global equilibrium surfaces in three dimensions are
described by elementary functions in closed form for models
of loaded arches, struts and shells. They are computed and
displayed graphically, in a form which shows their relation
with the local equilibrium surface generated by the cusp
catastrophe potential. Global bifurcation sets and equilib-
rium paths are also displayed. Some pros and cons of
finite-dimensional modelling are discussed. A parabolic
pure catastrophe machine is described.

AMS(MOS) Subject Classification - 58E15, 58F05, 70.49, 73.49, 93D05.

Key Words - Bifurcation, Catastrophe, Buckling, Elasticity,
                        Stability, Equilibrium, Structures.

Work Unit Number 3 - Applications of Mathematics

SOME GLOBAL EQUILIBRIUM SURFACES

M. J. Sewell

The concept of the 'equilibrium surface' was introduced by Sewell [2] in a paper written ten years ago. The context was the stability of engineering structures, and papers were appearing at that time which had the effect of emphasizing only particular equilibrium paths on the surface, or their projections onto certain planes. My object was therefore to provide a more complete perspective in which to embed these paths and projections, and so to make fully explicit the geometrization of stability analysis in terms of a 'stability boundary' defined on the smooth equilibrium surface.

Specifically, if the description of a system contains a scalar function

$$V(x_i; \lambda_\alpha) \tag{1}$$

of n 'behaviour' variables x_i and k mathematically assignable 'control parameters λ_α', the n equations

$$\frac{\partial V}{\partial x_i} = 0 \qquad (i = 1, \ldots, n) \tag{2}$$

relating these variables and parameters describe an 'equilibrium surface' in the $(n+k)$-dimensional space spanned by all the n x_i and the k λ_α. The set of points on the surface for which the $n \times n$ Hessian determinant

$$\left| \frac{\partial^2 V}{\partial x_i \partial x_j} \right| = 0 \tag{3}$$

was called the 'stability boundary'. A local minimum of V with respect to the x_i at fixed λ_α is taken to imply stability. The terminology is loaded towards the mechanics context, in which behaviour variables are generalized configuration coordinates, and control variables are such things as loads, moduli, dimensions, position of loads, and imperfection measures. In the purely mathematical literature, such as Morse theory, points satisfying (2) are called 'critical points' of V, and 'degenerate critical points' when (3) holds as well. The relevance of the 'stability' connotation really depends on the properties of time-differential equations describing the motion of the system off the equilibrium surface — these are given in [2] in the case of a damped conservative system, and also in two types of rotating system.

The advent of elementary catastrophe theory (Thom [1], [2]) has very much widened the interest in equations (1) - (3), serving in particular to re-emphasize the numerous contexts in which they appear besides the mechanics one. A principal result of catastrophe theory specifies the local shape of the so-called 'bifurcation set' in the λ_α-space. This bi-furcation set is the projection of the stability boundary onto the control space, and is obtainable in principle by eliminating all the x_i from (2) and (3). An associated requirement is that (1) be 'generic', i.e. that its local form would not be significantly altered by the introduction of more control variables. Associated dynamical equations can vary with the con-text, and can even describe 'slow flows' on the equilibrium surface in addition to 'fast flows' off it, as in Zeeman's [1] model of the heartbeat.

It seems desirable that the beginner, before getting to grips with these more sophisticated ideas of 'local', 'generic' and 'significantly altered' should see some very concrete examples of global equilibrium surfaces.

I present here three computed global equilibrium surfaces, each in three dimensions, for models of typical engineering structures. The global equations are obtained in simple closed form in terms of trigonometric functions, and plotted by computer. This allows one to see easily how the local results are embedded within the global, and therefore what the mathematical limitation of a local result might be. The pictures also offer an immediate understanding of how various cross-sectional equilibrium paths, different because not all mathematical controls are easily varied physically, are all contained in the unifying concept of the equilibrium surface. They also show global bifurcation sets as projections.

On the other hand, these models have the physical limitation that they only give a qualitative and local indication of the buckling behaviour of real structures, because in the latter other effects such as higher modes would intervene to complicate the global pictures shown here. Therefore there are dangers in allowing such models to acquire a life of their own, before addressing oneself rather soon to the differential equations describing the real structures. Budiansky [1], Hutchinson [2] and Sewell [3] have given recent reviews of the formulation and solution of real buckling problems. But spring models have often found an initial role in engineering

-3-

research in attempting to elucidate exactly that qualitative local response which we can now see is also offered by catastrophe theory. A notable recent fusion of these two approaches is found in the Zeeman catastrophe machine, although its global solution (Poston and Woodcock [1]) is analytically complicated by comparison with the global solutions given here.

The examples which follow were prepared as part of a dynamic course for second year undergraduate mathematicians. Perhaps it will not be many years before material of this type can be used in sixth forms as examples of modelling. Equations (1) - (3) provide an easy entry into other applied subject areas, for example whenever one can interpret the x_i as mode amplitudes. Of course this is to ride upon the backs of those who have taken the trouble to solve the underlying differential equations, and it is an approach which may be more suited to an expositor than to a researcher committed to a single area.

Equation and figure numbering begins anew in each of the following Sections.
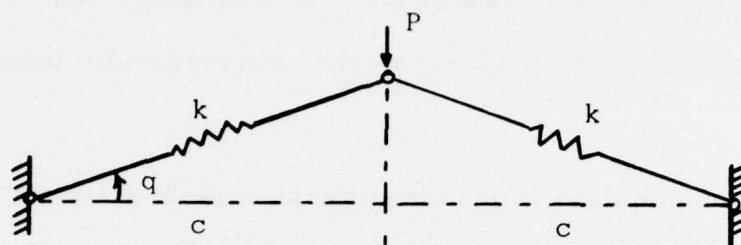
Shallow Arch or Spherical Cap Model

Figure 1. Model of shallow arch or spherical cap

The lid of a biscuit-tin (or beer-can) can be regarded as being ap-
proximately a very shallow spherical cap supported on a circular hinge
round its edge. When pressed transversely in the centre from the convex
side it will suddenly 'snap-through' the plane of the hinge, to a second
**equilibrium position under zero load but with the opposite concavity. It
can then be made to snap back by pressing from the opposite (i. e. new**
convex) side. If the unloaded lid is shallow enough, the effect can be
described entirely in terms of axisymmetric configurations, without re-
quiring an asymmetric mode. Certain older types of oil-can rely on such
snap-buckling to eject the oil, and then to take in air. The effect was
long known as oil-canning.

A mathematical model can be based on the plane structure shown in
Figure 1. Two equal rods are supposed to remain straight but have constant

longitudinal elastic modulus k . They are smoothly hinged to two pivots

fixed at a distance 2c apart, and they are joined at a third pivot which

can move on the perpendicular bisector of the first two, in the plane of the

paper only. A transverse dead load P acts symmetrically at the third

pivot, so that it may be balanced by the compression (or tension) in the

two rods.

The configuration is described by the angular deflection q of the

rods from their collinear position, with

$$-\frac{\pi}{2} < q < \frac{\pi}{2} \ .$$

Symmetry suggests that under zero load, one unstable and two stable

equilibrium configurations will be found, namely

$$q = 0, \ \pm \alpha \ \ \text{at} \ \ P = 0$$

respectively. The angle $\alpha \geq 0$ is intrinsically assigned in advance for

each given shell, and serves to specify upper and lower 'natural states'

$q = \pm \alpha$. The 'depth' of the shell is then adequately defined by

$$a = 1 - \cos \alpha \ ,$$

$$0 \leq a < 1 \ .$$

The total potential energy of the system in a general position under dead

load is

$$2 \cdot \tfrac{1}{2} k \left(\frac{c}{\cos \alpha} - \frac{c}{\cos q} \right) - P(c \tan \alpha - c \tan q)$$

with respect to the upper natural state as datum. Removing the additive

constant $P c \tan \alpha$, dividing by the fixed positive constant $2kc^2$, and writing $p = P/2kc$ leaves the normalized potential energy

$$V(q, p, a) = \frac{1}{2}\left(\frac{1}{1-a} - \frac{1}{\cos q}\right)^2 + p \tan q \ . \tag{1}$$

This depends on one behaviour variable q, and two control variables p and a. They are control variables in the mathematical sense of being independently assignable parameters, even though for a given shell (fixed a) only p is accessible to physical variation in a single 'test', in the range

$$-\infty < p < \infty \ .$$

The following analysis thus refers to a <u>family</u> of shells specified by a-values in the stated range. Given the mathematical model based on Figure 1, the global analysis can first be carried through without insisting on a shallow shell (small a) or small deflections (small q).

Eventually, to obtain a qualitative idea of the axisymmetric response of real shallow shells before asymmetric deflection modes intervene, it will be necessary to introduce the approximation of small α and therefore

$$\text{small } a \simeq \tfrac{1}{2}\alpha^2 \ .$$

Differentiation of the normalized potential energy shows that

$$\frac{\partial V}{\partial q} = \frac{1}{\cos^2 q}\left[p - \sin q\left(\frac{1}{\cos \alpha} - \frac{1}{\cos q}\right)\right] \ ,$$

$$\frac{\partial^2 V}{\partial q^2} = 2 \tan q \frac{\partial V}{\partial q} + \frac{1}{\cos^4 q}\left[1 - \frac{\cos^3 q}{\cos \alpha}\right] \ .$$

-7-

Since $\cos q > 0$ the equation of the equilibrium surface $\partial V/\partial q = 0$ in q, p, a-space is

$$p = \sin q(\frac{1}{1-a} - \frac{1}{\cos q}) \ . \tag{2}$$

The stability boundary is those points on the equilibrium surface where $\partial^2 V/2q^2 = 0$ also, i.e. where $\cos \alpha = \cos^3 q$ also. Thus the stability boundary is the smooth curved line

$$p = \tan^3 q, \quad 1 - a = \cos^3 q \ . \tag{3}$$

The bifurcation set in the control plane is obtained by eliminating q from these two equations, giving the projection of the stability boundary onto the control space. In the specified a- and q-domains it is only necessary to consider one real $\cos q = (1-a)^{1/3} > 0$ and two real roots $\sin q = [1 - (1-a)^{2/3}]^{\frac{1}{2}}$ of opposite sign, leading to the global equation

$$p = \frac{[1 - (1-a)^{2/3}]^{3/2}}{1-a} \tag{4}$$

of the bifurcation set. It is also possible to regard equations (3) as a regular parametric version of the bifurcation set, which can therefore be generated numerically by treating q as this parameter. In fact to plot the bifurcation set with elementary tools such as tables and/or slide rule, fewer operations are required if the parametric version (3) is used instead of the explicit version (4) (four operations instead of six). The bifurcation set (4) is shown in Figure 2. Exactly the same global bifurcation set, but in different control variables, arises later in a model of imperfection-sensitive shell buckling.
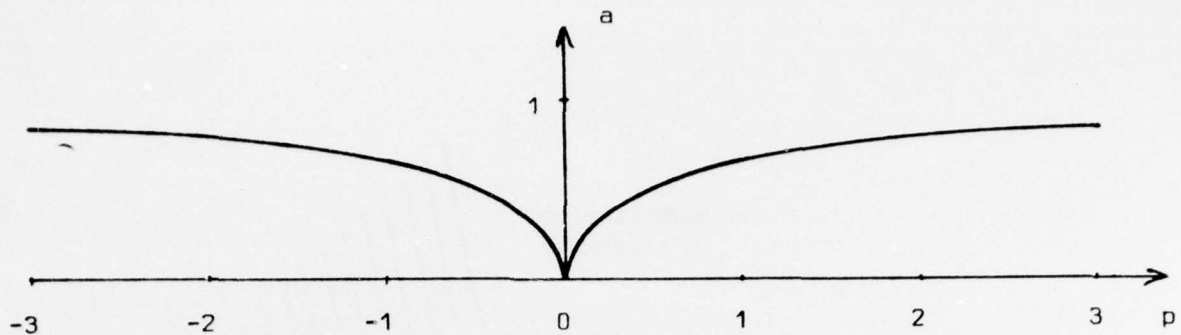
Fig. 2 Bifurcation set for the arch model

The complete equilibrium surface (2) is a smooth folded surface,

drawn in Figure 3 in the most significant domain of q, p, a-space by

computing the cubic-like cross-sections at successive fixed values of a .

The stability boundary (3) is the fold-line on the surface, separating un-

stable (broken cross-section) from stable (unbroken) equilibrium points,

and its projection onto the p, a-control plane is the cusped bifurcation

set shown again in Figure 3.   In other words, the fold-line is

the locus of points on the surface where the tangent-plane is parallel to

the q-axis. The envelope of such tangent planes where they intersect

the control plane is the bifurcation set. Figure 3 also shows intercepts

of the plane p = 0 with the surface (paths of unloaded equilibrium - cf.

Figure 5), with the control plane, and with the plane $a = \frac{1}{2}$. Notice

that different scales have had to be used on the three orthogonal cartesian

axes of Figure 3, but equal scales are retained in the plane diagrams of
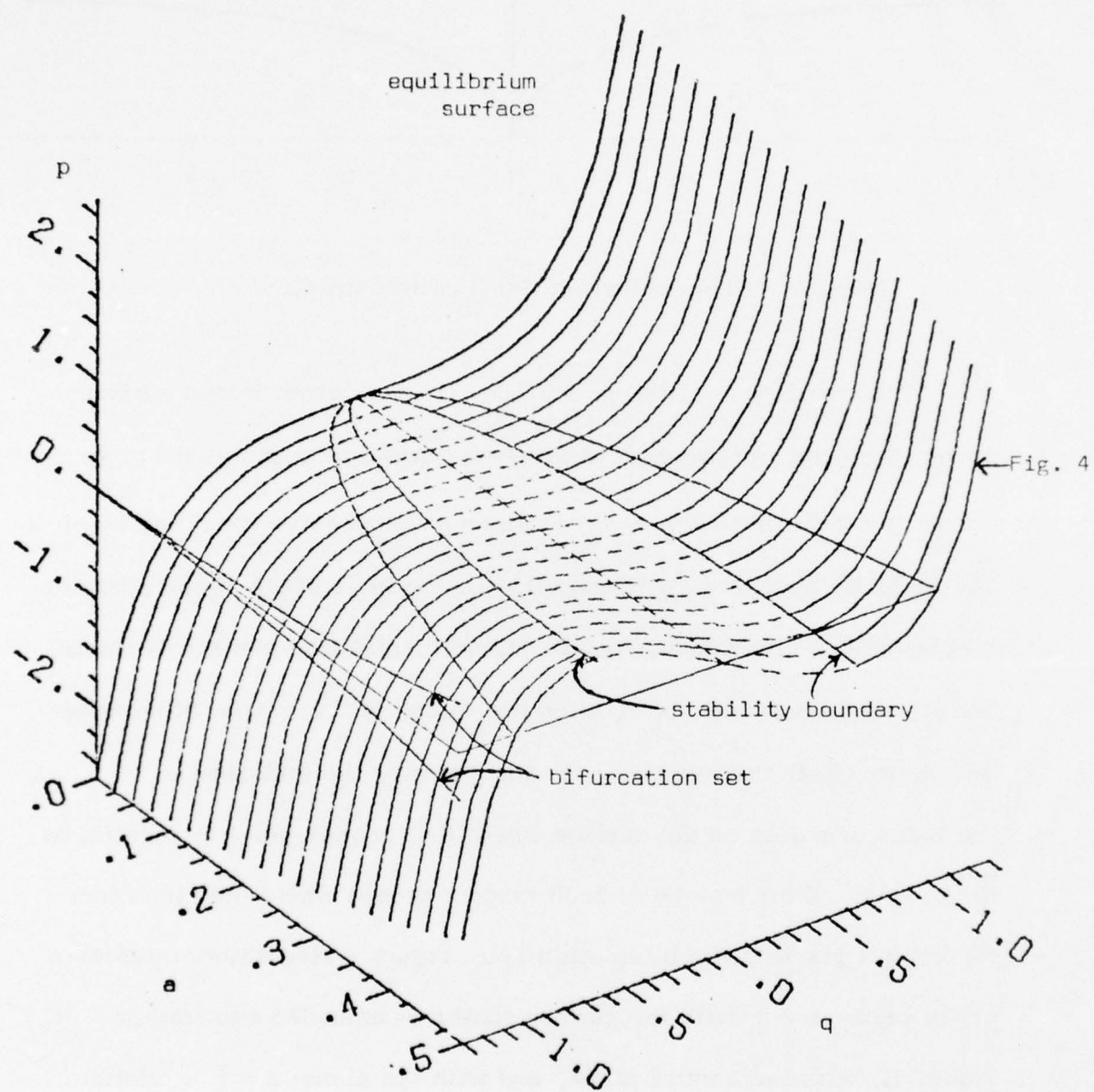
Figures 2, 4 and 5.

Fig. 3. Equilibrium surface and bifurcation set for the arch model.

The stability boundary itself actually consists of equilibrium points which are unstable 'almost everywhere' (except at the origin, in fact), because on this fold-line $\partial^3 V/\partial q^3$ has the values

$$\frac{3 \sin q}{\cos^5 q} \neq 0 \quad \text{unless} \quad q = 0 .$$

Since $\partial^2 V/\partial q^2 < 0$ in the broken-lined reverse-sloped part of the equilibrium surface, the totality of unstable equilibrium points are within and on this fold-line (except the origin itself). Elsewhere $\partial^2 V/\partial q^2 > 0$, and so the two full-lined open regions of the surface outside the fold (connected only at the origin) make up the totality of stable equilibrium points.

In a single test of a given shell, the depth a is fixed and the dead load p is varied quasi-statically. Those equilibrium paths on the surface which are of most physical interest are therefore those formed by its cross-sections with planes a = constant, as drawn in Figure 3. A typical such path is shown in Figure 4, the full line being stable equilibria and the dashed line being unstable equilibria. In particular this confirms the above-mentioned expected solutions under load p = 0. Quasi-static loading from either natural state in the direction of the single arrows will bring the system to the stability boundary where also the equilibriating load is a local maximum or minimum. Since the stability boundary is itself unstable, dynamical snap-buckling must take place from there to the 'energy basin of attraction' associated with another finitely distant stable
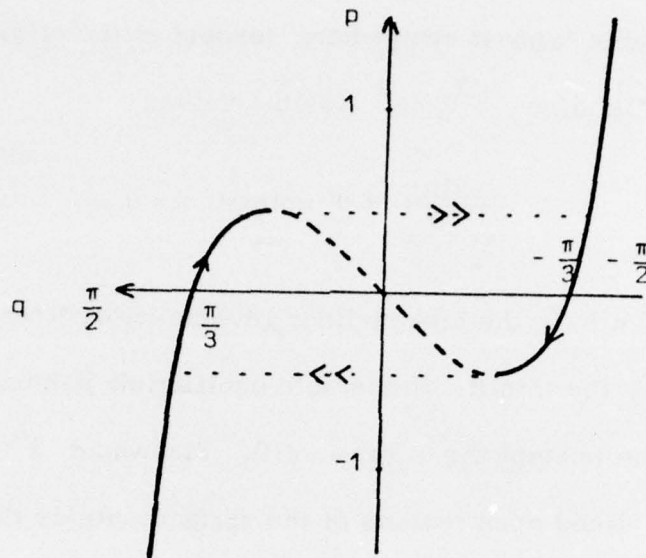
-11-

Fig. 4 Equilibrium path for a given shell $(a = \frac{1}{2} \Rightarrow \alpha = \frac{\pi}{3})$

equilibrium, as indicated by the double arrows in Figure 4. The oil-canning

mechanism is represented by the illustrated hysteresis cycle.

Such snap-buckling can therefore be represented in Figure 3 by a

dynamic jump in q, across from any given p and a on the fold-line.

In the control plane the bifurcation set is the 'failure locus', at which such

buckling can be induced by moving the control point (at fixed a) across

from the inside towards the outside of the cusp-shaped region.

Perpendiculars erected in Figure 3 from the control plane will in-

tersect the equilibrium surface in either one point (if from outside the cusp)

or three points (if from inside the cusp). The outside of the bifurcation set

therefore also delimits the range of control parameters for which <u>uniqueness</u>

of the equilibrium solution is assured.

The cross-section of the equilibrium surface at zero load $p = 0$ is
shown in Figure 5. As a increases from zero in (2), three branches of
equilibrium path emerge from the origin, with two stable and one unstable
as indicated. Such branching will not be observable in a test on a <u>single</u>
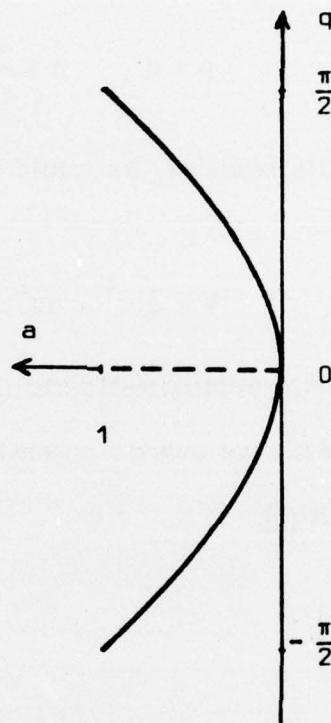shell, however.

Fig. 5   Branched equilibrium paths in the plane $p = 0$

For the case of a shallow shell, it is easy to note the approximate
form taken by the foregoing global equilibrium analysis for small $a \geq 0$.
The bifurcation set (4) becomes

$$p = (\frac{2a}{3})^{3/2} [1 + \frac{5}{4} a + \theta(a^2)] \ .$$

Locally this is the two-thirds power law cusp

$$27p^2 = 8a^3 \ .$$

It is evident from (3) that p and q are also small on the stability boundary, since the local form of this fold-line is

$$p = q^3, \qquad a = \frac{3q^2}{2} \ .$$

This is the same stability boundary as would have emerged if the quartic potential

$$V = \tfrac{1}{4} q^4 - aq^2 + 2pq$$

had been used as the local approximation to (1). This connection of the shallow shell problem with the quartic potential of Thom's cusp catastrophe was described by Sewell [1].
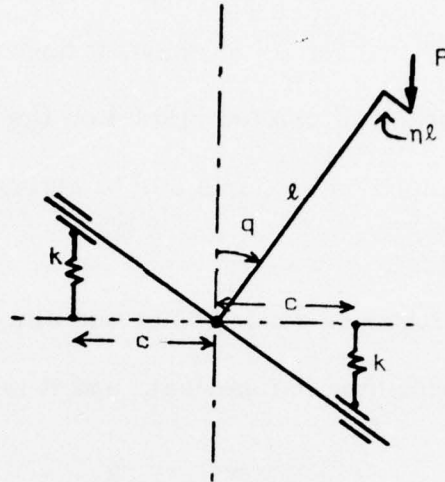
-14-

Strut or Compressed Plate Model

Fig. 1   Model of eccentrically loaded strut

Axially loaded struts, and flat rectangular plates compressed in their plane, belong to a class of structures which retain some static strength even after their classical compressive buckling loads, such as the Euler load, have been exceeded. This is because the straight configuration can branch stably and quasi-statically into a buckled configuration as the load increases, in a manner which is not sensitive to the size or character of small imperfections in geometry or loading. The elastica is the most famous example, and its large deflection equilibrium solutions have been studied intensively.

The theoretical model shown in Figure 1 consists of a rigid T-piece having a small flange of length $\eta\ell$ welded perpendicularly to the main stem of length ℓ . The flange is to represent imperfections, and a vertical dead

load P is applied at the end of it.   Rotation about a fixed smooth pivot
at the root of the T is restrained by two linear elastic springs of modulus
k, which exert vertical forces at constant horizontal separation 2c, via
a suitable arrangement of pivoted sliders on the arms of the T . The moment
of P is thus balanced by a couple due to spring forces having lines of
action fixed in space.

The configuration is described by the single angle q measuring de-
flection of the model from the vertical, and it is adequate to suppose

$$-\frac{\pi}{2} < q < \frac{\pi}{2} .$$

The entire behaviour is in the plane of the paper only. In the absence of
imperfections ($\eta = 0$) it is obvious that the vertical position $q = 0$, in-
volving zero extension of the springs, could be in equilibrium (not neces-
sarily stable) under arbitrary load P .

The total potential energy of the system in a general position under
dead load is

$$2 \cdot \tfrac{1}{2}k(c \tan q)^2 - P(\ell - \ell \cos q + \eta \ell \sin q)$$

with respect to the vertical position. Dividing by the fixed positive con-
stant $2kc^2$ and writing $p = P\ell /2kc^2$ leaves the normalized potential energy

$$V(q, p, \eta) = \tfrac{1}{2} \tan^2 q - p(1 - \cos q + \eta \sin q) . \tag{1}$$

This depends on one behaviour variable q, and two control variables p
and η . As in the arch problem p is effectively the dead load, assignable
in the range

$$-\infty < p < \infty \quad .$$

The other control η is again ostensibly an assignable geometry variable, and it will be enough to suppose that

$$-1 \ll \eta \ll 1 \quad .$$

The real role of the η-term in (1), however, is to try to represent an arbitrary 'perturbation' of the form of the potential from that for the 'perfect' system (having $\eta = 0$ in (1)); and so to convert from the supposedly non-generic perfect system to a hoped-for generic description of the system, now containing imperfections. It can be seen that η only appears in (1) in combination with p as $p\eta$, the couple induced by imperfections in the vertical 'straight' configuration as soon as load is applied. For the second assignable control parameter it may therefore be more appropriate to use $p\eta$ rather than η.

Differentiation of the potential (1) gives

$$\frac{\partial V}{\partial q} = \frac{1}{\cos^3 q} [\sin q(1 - p \cos^3 q) - p\eta \cos^4 q] \quad ,$$

$$\frac{\partial^2 V}{\partial q^2} = -\tan q \frac{\partial V}{\partial q} - \frac{1}{\cos q} [p - \frac{4 - 3\cos^2 q}{\cos^3 q}] \quad .$$

Since $\cos q > 0$ the equation of the equilibrium surface $\partial V / \partial q = 0$ in $q, p, p\eta$-space is

$$p\eta \cos^4 q = \sin q(1 - p \cos^3 q) \quad . \tag{2}$$

-17-

The stability boundary on this surface, where $\partial^2 V/\partial q^2 = 0$ as well, is the smooth curved line

$$p = \frac{4 - 3\cos^2 q}{\cos^3 q}, \quad p_\eta = \frac{-3\sin^3 q}{\cos^4 q} . \qquad (3)$$

The bifurcation set in the p-p_η control plane is generated by these same equations (3), with q regarded as a regular parameter instead of a third coordinate. In principle q could be eliminated from this parametric form to obtain an explicit expression for the curve in terms of the control variables alone. But this procedure seems even less worthwhile, either analytically or numerically, then was the case with equation (4) of the arch model.

In seeking to plot the global equilibrium surface (2) explicitly, it is natural in this example to look first at its intersection with the plane of zero imperfection $p_\eta = 0$. This gives the two equilibrium paths

$$q = 0 \quad \text{and} \quad p = \frac{1}{\cos^3 q}$$

intersecting at the 'Euler load' bifurcation point $p = 1$, $q = \eta = 0$ as shown in Figure 2. Again the full lines represent stable equilibrium (where $\partial^2 V/\partial q^2 > 0$), and the dashed line unstable equilibrium (where $\partial^2 V/\partial q^2 < 0$). Thus as the dead load p is increased from zero (or below) in the absence of imperfections, the undeflected equilibrium of the strut is stable for $p < 1$, and unstable for $p > 1$. It happens that the bifurcation point itself is also stable (because $\partial^2 V/\partial q^2 = \partial^3 V/\partial q^3 = 0$, $\partial^4 V/\partial q^4 > 0$ there), and

-18-

so as p increases through $p = 1$ the system can evolve stably and quasi-statically onto the deflected equilibrium path.

In this way Euler struts and certain compressed plates exploit the fact that this bifurcation point is also the _only_ point on the stability boundary where the equilibrium is actually found to be stable when higher
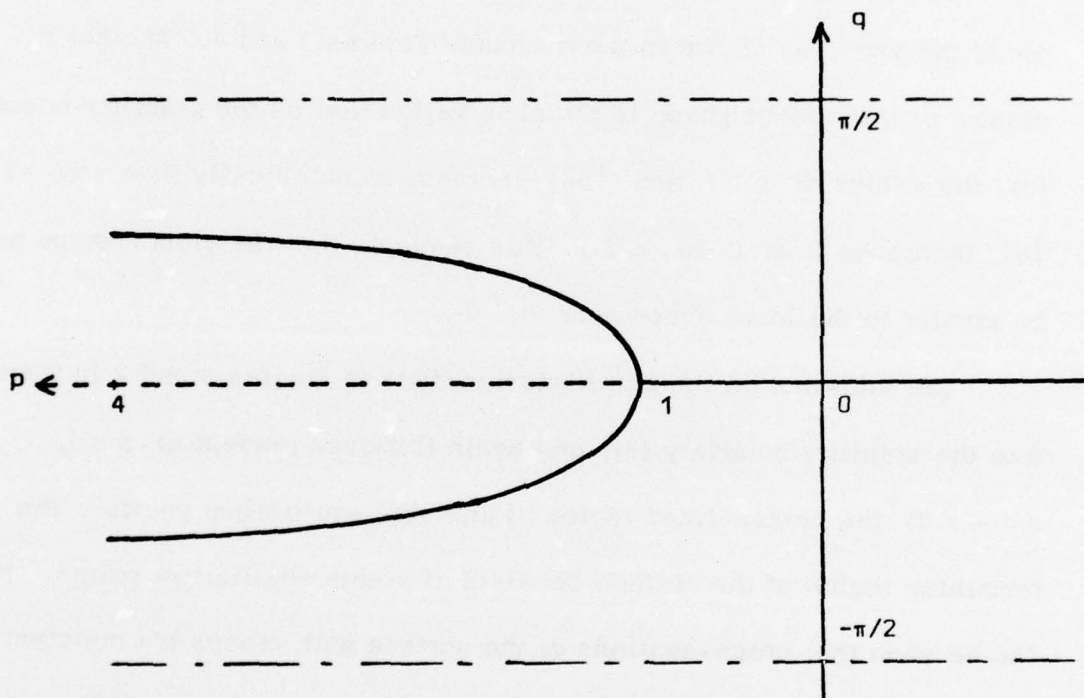

Fig. 2   Branched equilibrium paths for zero imperfection

terms in the potential energy are examined.   In fact, just as for the arch model, the points of the stability boundary represent unstable equilibrium 'almost everywhere' (because $\partial^2 V/\partial q^2 = 0$, $\partial^3 V/\partial q^3 \neq 0$ on it unless $p = 1$).   Thus such Euler buckling of perfect struts and plates is a quasi-static phenomenon in contrast to the dynamic snap-buckling exhibited by arches, spherical caps and other kinds of shell structures.

-19-

On the other hand, Figure 2 is qualitatively the same as Figure 5 of the arch model. The only essential difference is the interpretation of the single control variable in the two diagrams. This similarity helps one to see that the complete equilibrium surface (2) for this strut model, in q, p, p_η-space, is a smooth folded surface of exactly the same qualitative shape as that already obtained for the arch, but with different variables along the axes, as shown in the computed Figures 3 and 4. Another indicator of this global shape is the observation that on the stability boundary (3), the values of $p - 1$ and $|p_\eta|$ increase monotonically from zero as $|q|$ increases from 0 to $\pi/2$. This suggests that the global shape will be similar to the local shape near $q = 0$.

The fold-line on the equilibrium surface in Figures 3 and 4 is therefore the stability boundary (3), and again it closes (except at $p = 1$, $q = \eta = 0$) the broken-lined region of unstable equilibrium points. The remaining region of the surface consists of stable equilibrium points. It can be seen that cross-sections of the surface with planes $p = $ constant for $p > 1$ would have the same qualitative shape as Figure 4 of the arch problem, except that p_η would now be the control variable in that plane. However, there might not be a convenient physical facility for varying the mathematical control η, representing imperfection, independently of the load p.

This type of distinction between mathematical and physical controls, in problems which have substantially the same mathematical equilibrium
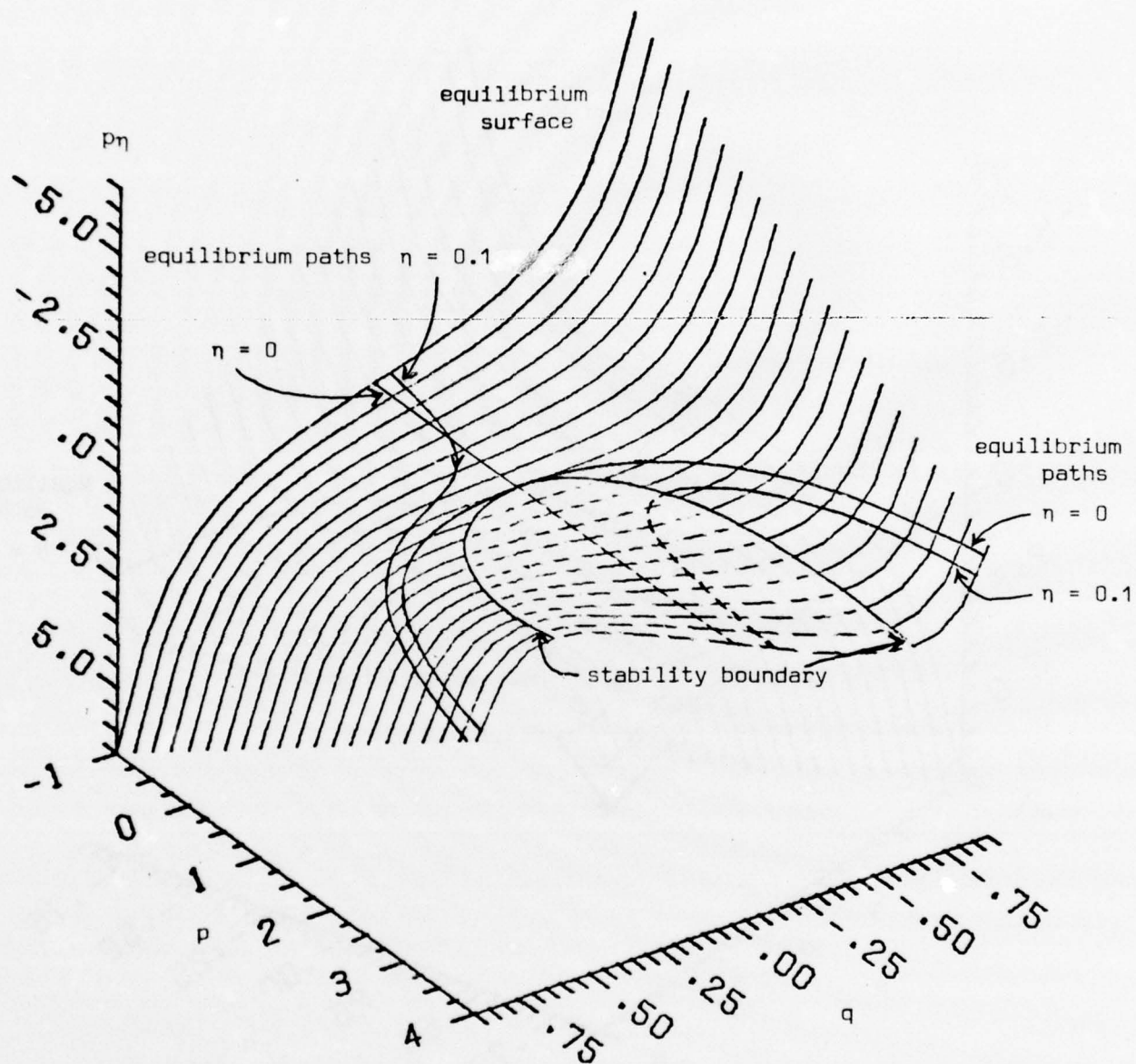
Fig. 3. Equilibrium surface and stability boundary for the strut model, with equilibrium paths for perfect (η = 0) and imperfect (η = 0.1) struts.
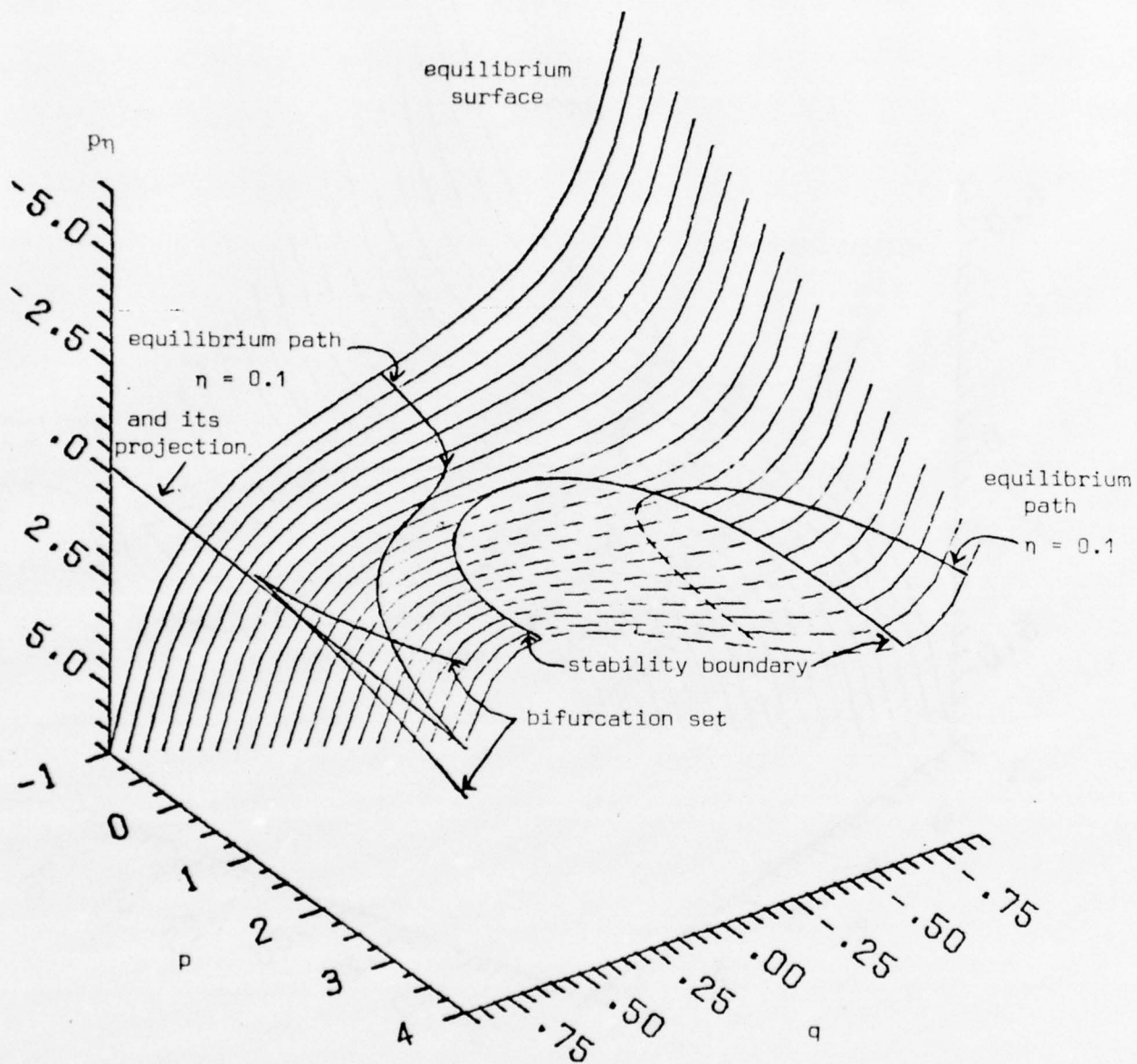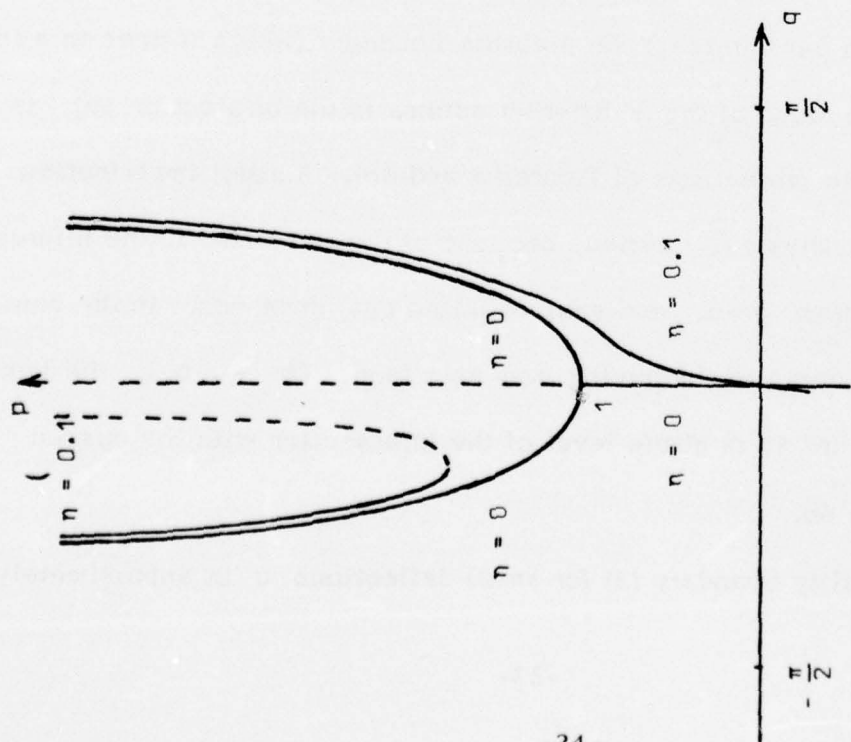
Fig. 4. Equilibrium surface and bifurcation set for the strut model, with equilibrium paths for an imperfect strut η = 0.1.

surface, implies a distinction between the type of equilibrium paths which can be physically realized on that equilibrium surface.

The bifurcation set is shown in Figures 4 and 5b as the projection of the fold-line onto the control space. Again the outside of it delimits the range of control parameters for which uniqueness of the equilibrium solution is assured. Evidently the lowest load at which uniqueness can fail is the Euler load $p = 1$. Also shown on Figures 4 and 5b is the linear projection $p_\eta = 0.1p$ onto the control space of equilibrium paths for which $\eta = 0.1$.

Physically realizable equilibrium paths for the imperfect model would be obtained by intercepts of the equilibrium surface with planes $\frac{p_\eta}{p}$ = small constant in Figures 3 and 4. Each intercept has two disjoint parts, only the arrowed one can begin from zero load, and it is only the other one which can intercept the stability boundary (which it does in a load minimum. The locus of these different minima is the bifurcation set, as illustrated in the projections of Figures 4 and 5b). A small imperfection is therefore not physically serious because of the rapid rise in the bifurcation set curve from $p = 1$, and snap buckling can never occur in the continuous equilibrium path beginning from zero load. For $\eta = 0.1$, the load minimum in Figure 5a is at the level of the intersection with the cusped curve in Figure 5b.

The stability boundary (3) for small deflections q is approximately

-23-

(b) Bifurcation set, and loading path for $\eta = 0.1$
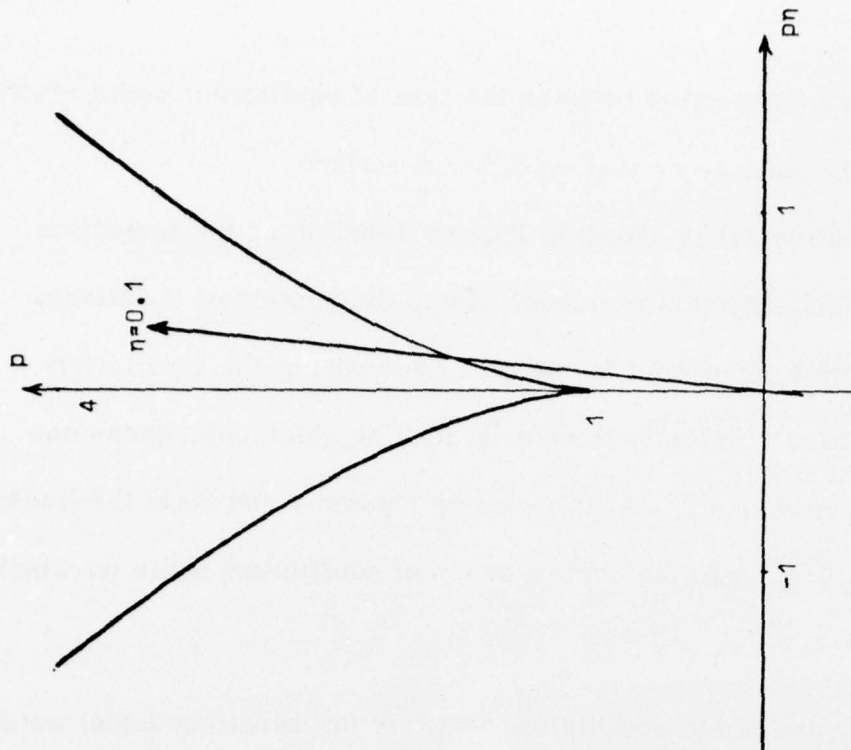
(a) Equilibrium paths for $\eta = 0$ and $\eta = 0.1$

Fig. 5 Projections of the equilibrium surface for the strut model

$$p - 1 = \frac{9}{2} q^2, \quad p\eta = -3q^3 \, ,$$

so that by elimination of q the local shape of the bifurcation set is again the two-thirds power law cusp

$$81(p\eta)^2 = 8(p - 1)^3 \, .$$

This is the same stability boundary and bifurcation set which would have emerged if the quartic potential

$$V = \frac{3}{8} q^4 - \frac{1}{2} (p - 1)q^2 - p\eta q$$

had been used as the local approximation to (1). This quartic was given by Sewell [1], where it was remarked that this strut model offers an exact illustration of Thom's cusp catastrophe.
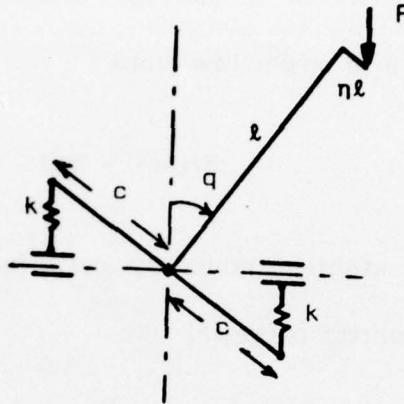
Shell Model

Fig. 1   Model for shell behaviour

Certain shell structures, such as axially loaded circular cylinders, or sufficiently curved cylindrical panels compressed parallel to their generators, have a classical bifurcation load in the absence of imperfection which can be a serious overestimate of their real resistance to buckling. This is because the straight configuration has only unstable equilibrium paths emanating from the classical bifurcation load, and the effect of these when generic imperfections are considered is to induce load maxima at only a fraction (perhaps $\frac{1}{3}$ or $\frac{1}{4}$) of the non-generic classical value.

The theoretical model in Figure 1 was analyzed by Sewell [2]. It is the same as the model for struts and plates, except in one key feature. The vertical lines of action of the restoring springs are no longer fixed in space, but are attached to fixed points on the arms of the T-piece, at a

given distance c along the arms from the pivot. The horizontal separation of the spring forces can now decrease with rotation, instead of remaining fixed as before. This makes the structure susceptible to sideways dynamic collapse early in a continuous equilibrium path beginning from zero load, in contrast to the model of the strut.

The extension of a spring is now c sin q instead of the previous c tan q, and this sole and apparently innocent analytical change has a radical effect, even on the small deflection analysis. (The interpretation of the constant c is different in the two models). The normalized potential energy becomes

$$V(q, p, \eta) = \tfrac{1}{2} \sin^2 q - p(1 - \cos q + \eta \sin q) \tag{1}$$

in the same domains as before. With cos q > 0, differentiation gives

$$\frac{\partial V}{\partial q} = \sin q \cos q - p \sin q - p\eta \cos q \ ,$$

$$\frac{\partial^2 V}{\partial q^2} = - \tan q \frac{\partial V}{\partial q} - \frac{1}{\cos q} [p - \cos^3 q] \ .$$

The <u>equilibrium surface</u> is therefore

$$p\eta = (\cos q - p)\tan q \tag{2}$$

and the <u>stability boundary</u> on it is the smooth curve

$$\eta = \tan^3 q, \quad p = \cos^3 q \ . \tag{3}$$

This is exactly the same global curve, but in different control variables, as was obtained for the stability boundary (3) in the arch problem.

-27-

Therefore, elimination of q can be carried out explicitly as before, in the range $-\pi/2 < q < \pi/2$, and leads to the global equation

$$\eta = \frac{[1 - p^{2/3}]^{3/2}}{p}$$

for the __bifurcation set__ in the p-η plane. Alternatively this bifurcation set could be plotted in p - $p\eta$ space as the symmetric curve

$$p\eta = [1 - p^{2/3}]^{3/2} \tag{4}$$

or via its parametric form $p\eta = \sin^3 q$, $p = \cos^3 q$. This curve is shown in Figure 2, and is the upper half of

$$(p\eta)^{2/3} + p^{2/3} = 1 .$$

The side cusps are the same as the cusp at $p\eta = 0$, $p = 1$, but are not actually attained because of the restriction to $|q| < \pi/2$.
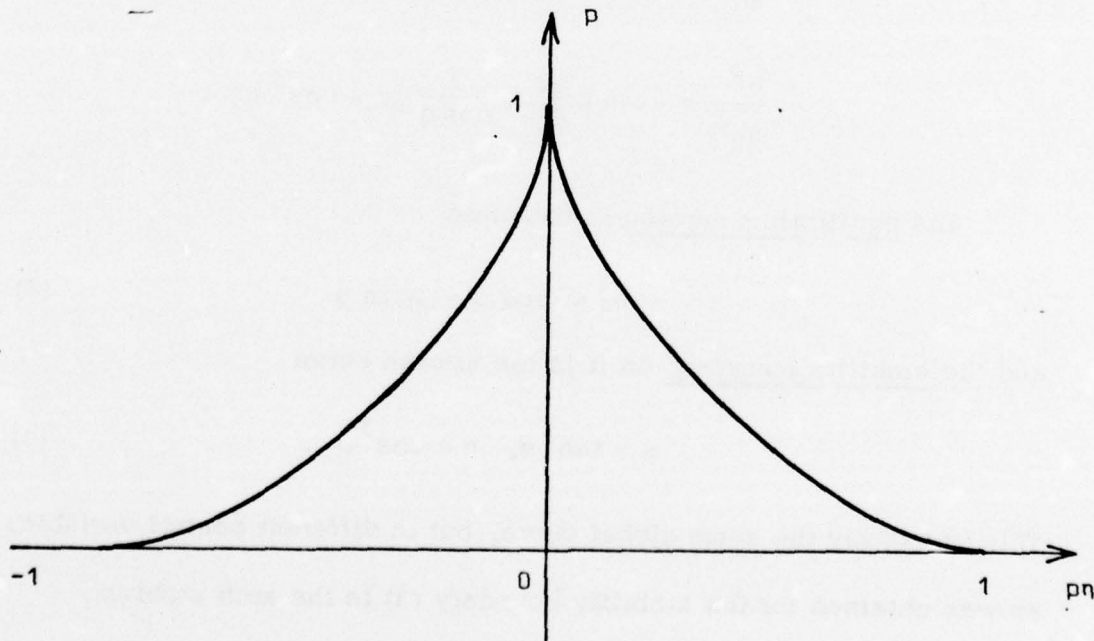

Fig. 2   Bifurcation set for shell model

The cross-section of the equilibrium surface (2) at zero imperfection $p_\eta = 0$ gives the two equilibrium paths

$$q = 0 \quad \text{and} \quad p = \cos q \ ,$$

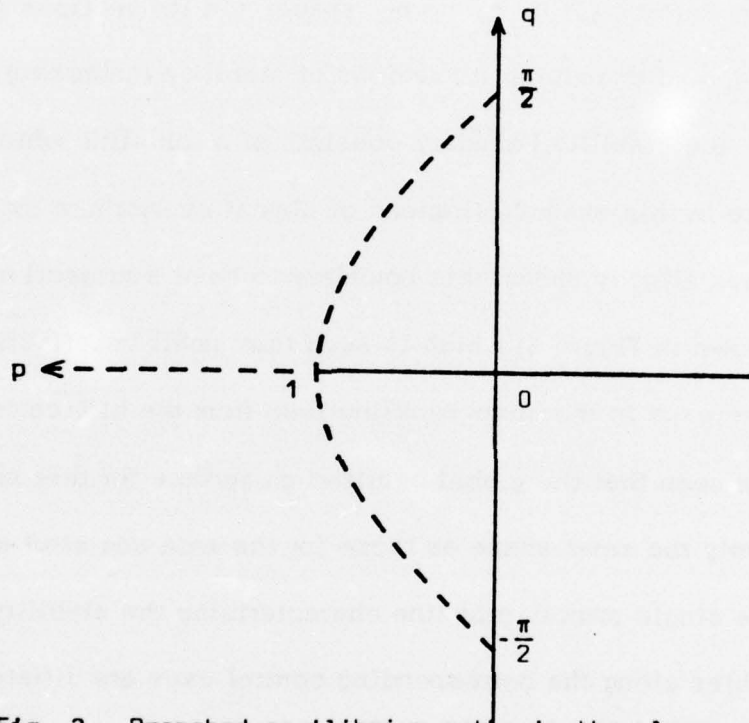intersecting at the bifurcation load $p = 1$, $q = \eta = 0$ as shown in Figure 3.

Fig. 3   Branched equilibrium paths in the plane $\eta = 0$

As the dead load is increased from zero or below in this example, the undeflected equilibrium of the model is stable for $p < 1$ and unstable for $p > 1$. By contrast with the strut model, the facility that the springs can now approach each other means that all the deflected equilibrium

-29-

configurations are unstable in the 'perfect' system, and so is the bifurcation point itself (because $\partial^2 V/\partial q^2 = \partial^3 V/\partial q^3 = 0$, $\partial^4 V/\partial q^4 < 0$ there).

This latter observation is the tell-tale sign, observed by Koiter [1], that the dynamic snap-buckling load is sensitive to imperfections.

This sensitivity is manifested graphically by computing the whole equilibrium surface (2) in q, p, p_η space, via its sections p = constant in Figure 4, and examining its regions of stability (unbroken) and instability (broken). The stability boundary consists of a fold-line which is unstable everywhere in this example (instead of almost everywhere as before). Figure 2 has already shown this boundary to have a projection on the $p - p_\eta$ space (shown in Figure 5) which is such that small imperfections p_η induce a large decrease in the snap-buckling load from the bifurcation value $p = 1$.

It is seen that the global equilibrium surface for this shell model is qualitatively the same shape as those for the arch and strut models, in having the single smooth fold line characterizing the stability boundary. The variables along the corresponding control axes are different in the three cases, and so are the distributions of stability and instability. These comparisons between the global equilibrium surfaces were described by Sewell [1].

Physically realizable equilibrium paths for the imperfect shell model can be obtained, as for the strut model, by intercepts of the equilibrium surface with planes $\frac{p_\eta}{p}$ = small constant in Figure 5. Each intercept again has two disjoint parts, but this time it $\underline{is}$ the branch (arrowed) beginning

-30-

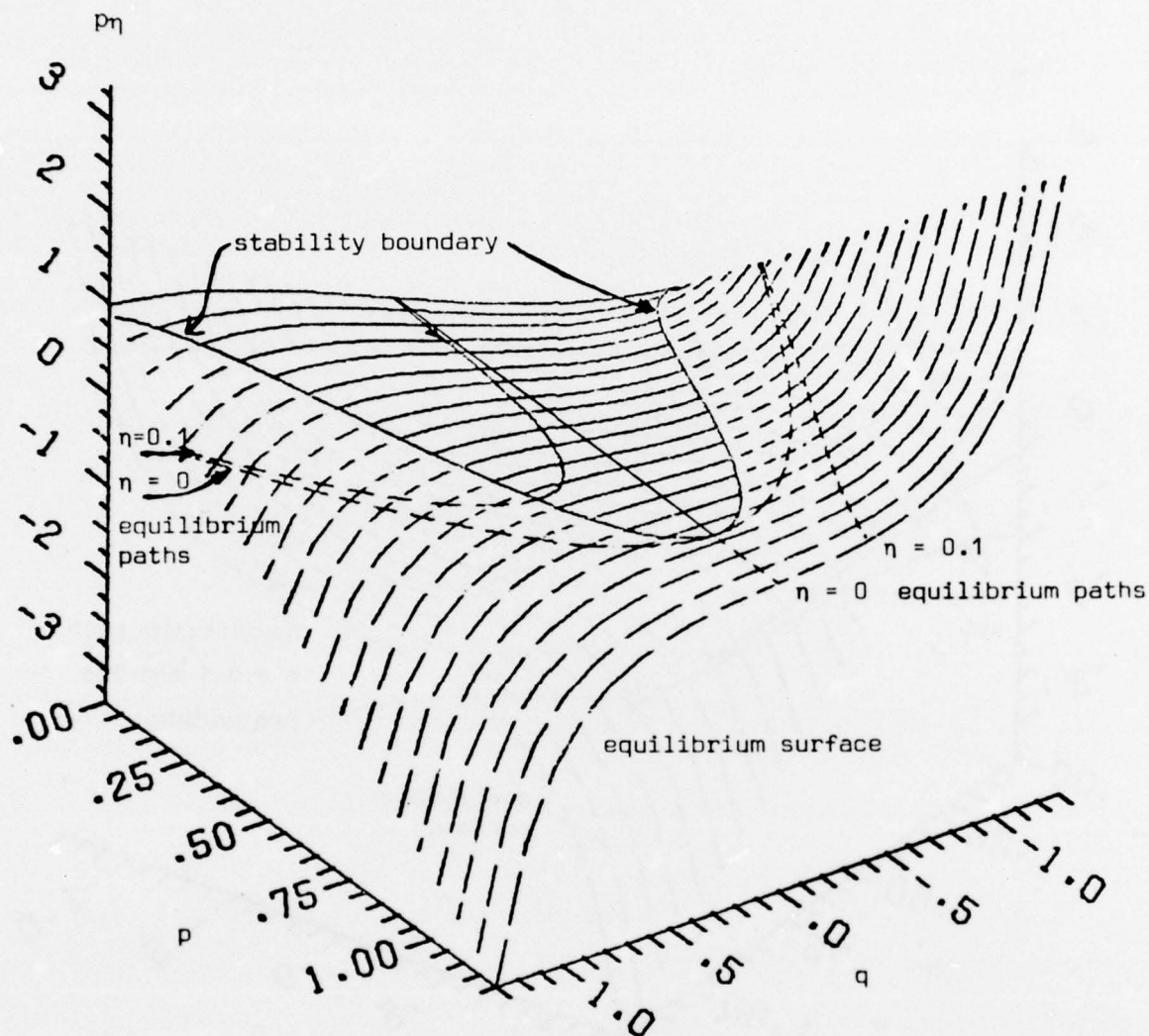Fig. 4. Equilibrium surface and stability boundary for the shell model,
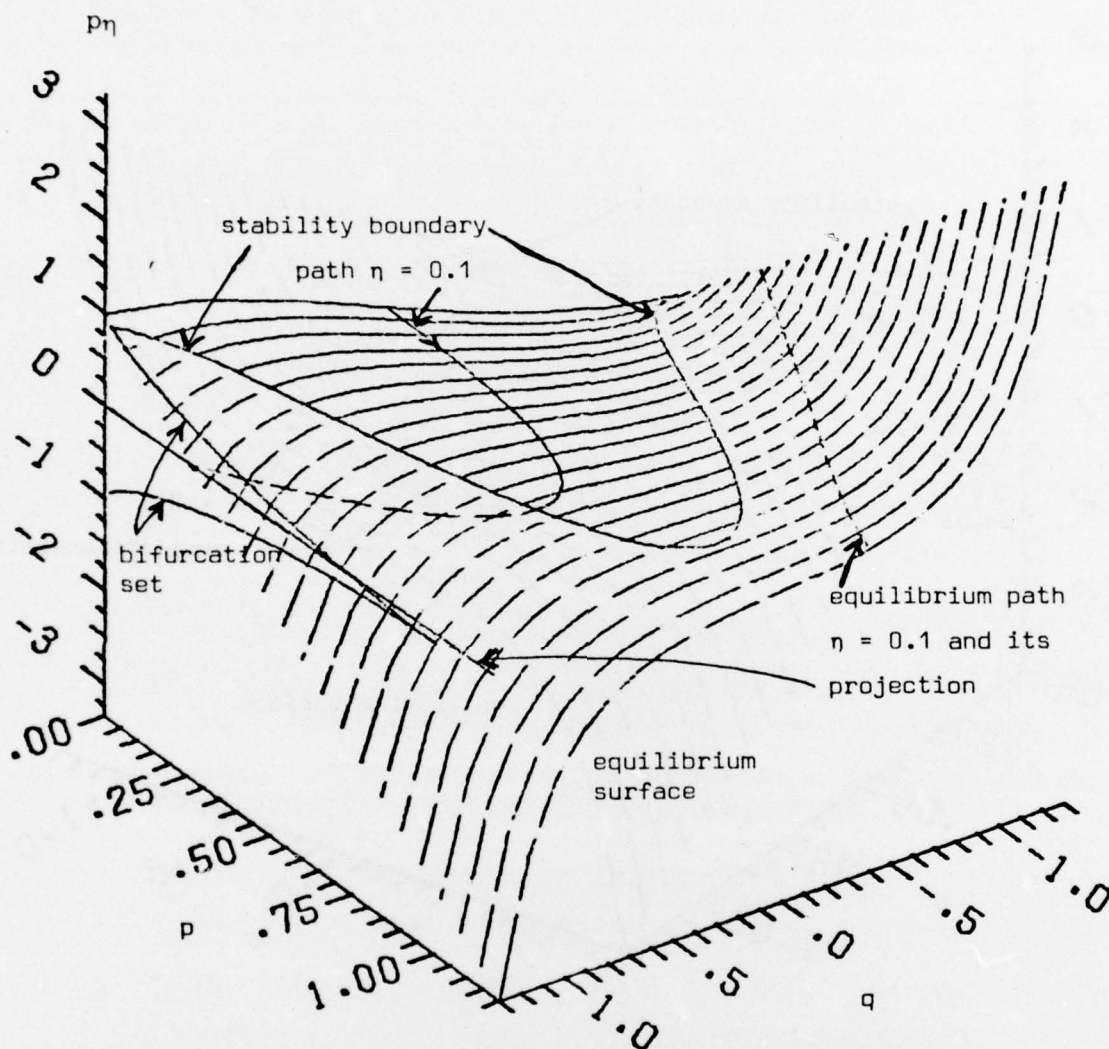with equilibrium paths for perfect (η = 0) and imperfect
(η = 0.1) shells.

Fig. 5. Equilibrium surface and bifurcation set for the shell model, with equilibrium paths for an imperfect shell $\eta = 0.1$.

from zero load which intercepts the stability boundary, and it does so at a load _maximum_. The locus of these different maxima is the bifurcation set, as illustrated in Figure 6b. A small imperfection is deleterious to the buckling strength because of the rapid drop in the bifurcation set curve associated with its vertical tangent at $p = 1$, and because this curve can be reached in a continuous equilibrium path beginning from zero load.

From the point of view of uniqueness, assigned values of the controls p and p_η outside the cusped curve imply unique but unstable equilibrium configurations. Inside the cusp curve, even for zero load and imperfection, there is no uniqueness but two unstable and one stable equilibria. Thus the shell model has no equilibrium configuration which is both unique and stable, in contrast to the strut model.

The stability boundary (3) for small deflections q is approximately

$$p - 1 = \frac{3}{2}\, q^2, \quad p_\eta = q^3 ,$$

so that the local shape of the bifurcation set is the two-thirds power law cusp

$$27 (p_\eta)^2 = -8(p - 1)^3 .$$

This is the same stability boundary and bifurcation set which would have emerged if the quartic potential (Sewell [1])

$$V = -\frac{1}{8}\, q^4 - \frac{1}{2}\, (p - 1)q^2 - p_\eta q$$

had been used as the local approximation to (1). The leading minus sign in this quartic accounts for the changeover in the stability distribution, as compared with the plus for strut model, and means that the model and its local bifurcation set exemplify the so-called 'dual' cusp catastrophe.

-33-
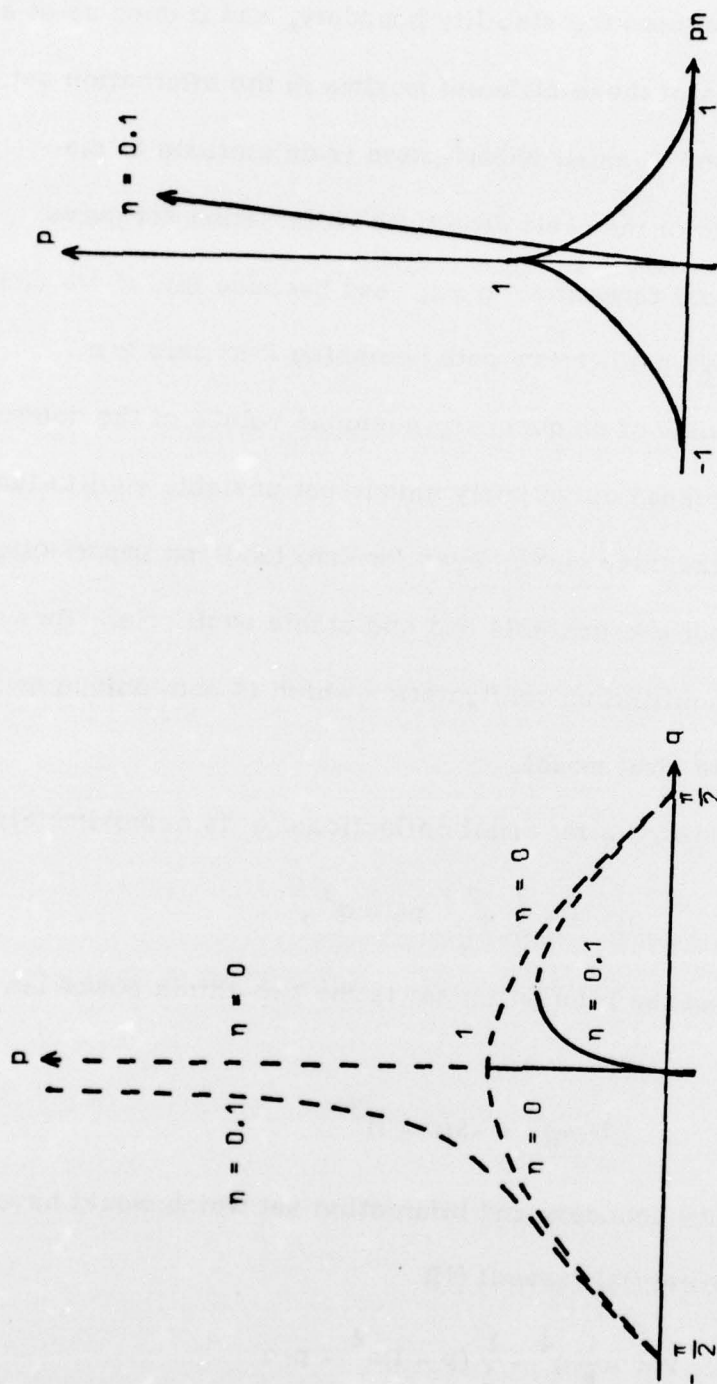
(b) Bifurcation set, and loading path for $n = 0.1$

(a) Equilibrium paths for $\eta = 0$ and $\eta = 0.1$

Fig. 6 Projections of the equilibrium surface for the shell model

A Pure Catastrophe Machine

Any sixth-former can actually construct and operate the following mechanical model of the cusp catastrophe. A plane lamina in the shape of his old friend the parabola $y^2 = 4x$ is made from a piece of stiff light card. It is enough to truncate the parabola at the ordinate $x = 8$. The card is to stand in a vertical plane with its parabolic edge resting on a horizontal table. The lateral stability required for this can be achieved by attaching it with three cardboard spacers of length 2 to another equal parabolic card, or preferably to a parabolic annulus since weight reduction is important. The annulus therefore acts like the secondary hull or out-rigger of a catamaran. A movable weight G is then attached to the first card, for example by a pair of small magnets gripping through the card with a force which must provide enough static friction to prevent their weight making them slide down the card. These practical details are the same as those suggested by Poston (see Poston and Stewart [1]) for an elliptical model.

The parabolic model is now that shown in Figure 1, with all the weight hopefully concentrated in the movable point G. To reduce the uniformly distributed card weight, it may be necessary to replace it with a second rigid parabolic annulus having a sheet of paper glued to it for G to ride upon. Suppose the contact point with the plane has parametric value t, where $x = t^2$, $y = 2t$ describes the parabola. By equilibrium the normal from t will pass through G. If G is outside the cusp-shaped envelope of the normals (as in Figure 1) there is a unique normal through G and

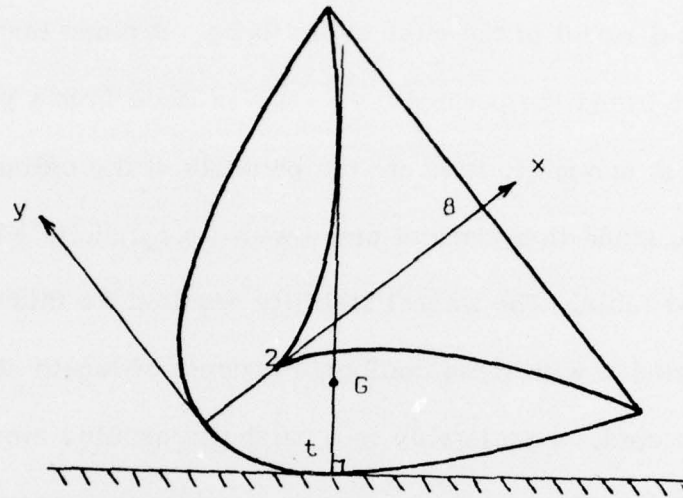therefore a unique (and stable) equilibrium configuration. But if G is

Fig. 1 Pure catastrophe machine

inside the envelope there are three normals from it to the parabola, and

their feet define one unstable and two stable equilibrium configurations.

The single parameter t is therefore the configuration or behaviour

variable of the system, and the coordinates x, y of the weight in the plane

are the two control variables. There is a folded equilibrium surface in the

three-dimensional t, x, y space whose stability boundary projects into the

cusped envelope in the x, y plane, as shown by Sewell [1, Figure 3]. The

potential energy when a unit weight G is at x, y and the contact point is

t, whether in equilibrium or not, is just the height

$$V(t; x, y) = [(x - t^2)^2 + (y - 2t)^2]^{\frac{1}{2}} + \text{constant} \qquad (1)$$

above any datum level. $V > 0$ if this datum is below the table top. Equilibrium is achieved at stationary values of this height as t moves around the parabola, i.e. where $\partial V/\partial t = 0$ or

$$t^3 - t(x - 2) - y = 0 \ . \tag{2}$$

This equation of the global equilibrium surface in t, x, y space is precisely the equation of the normal in the x, y plane to the parabola at t. That the shape of the surface is the same as the local versions of those for arch, strut and shell models can be seen from the following table of correspondences, in which Zeeman's adjectives are used to describe the two control variables.

	Machine	Arch	Strut	Shell
Behaviour	t	q	q	q
Splitting factor	$x - 2$	$2a$	$\frac{2}{3}(p - 1)$	$-2(p - 1)$
Normal factor	y	$-2p$	$\frac{2}{3}p\eta$	$-2p\eta$

Table: Corresponding behaviour and control variables

The stability boundary is the fold-line of points on the surface (2) where $\partial^2 V/\partial t^2 = 0$, i.e.

$$3t^2 - (x - 2) = 0 \ . \tag{3}$$

Elimination of t between (2) and (3) gives the bifurcation set

$$4(x - 2)^3 = 27y^2 \tag{4}$$

which is also the cusped envelope of normals shown in Figure 1. Envelope calculations require exactly this type of elimination.

-37-

Therefore the machine can be used to demonstrate a cusp catastrophe as follows. The weight G is moved quasi-statically (slowly) over the x, y plane from its position in Figure 1 to a point inside the cusp (Figure 2). Two new but distant equilibrium configurations have now become available, at t_2 (unstable) and t_3 (stable), in addition to the preferred t_1 (stable) which has been reached by the continuous quasi-static change from Figure 1.
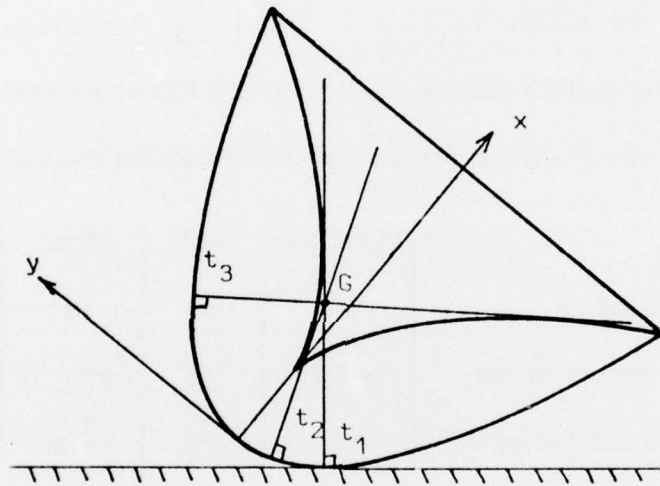
Fig. 2   Three equilibrium positions

Next G is moved outside the cusped region across the opposite side from that where it entered the region. As it leaves, the stable t_1 coalesces with the unstable t_2 as the equilibrium surface point reaches the stability boundary, and the system must suddenly jump to the energy basin of attraction surrounding the only remaining and stable configuration t_3. This is the catastrophe, manifested by the sudden jump in configuration as the parabola rolls over dynamically to allow G to come to rest vertically above t_3 instead of t_1.

-38-

This might be as pure a catastrophe machine as can be devised, in the sense that only the most trivial transformations are needed to put the physically derived expressions of (1) and (2) into the mathematically standard quartic and cubic forms respectively. Furthermore they are valid globally, and not only as local approximations.

It is worth noticing that any problem concerned with optimizing distance to a concave set of points might be available for reinterpretation as a gravitational catastrophe machine, since distance is equivalent to gravitational energy in the earth's field and because a convex boundary can roll on a table.

Concluding Remarks

It will be seen that I have not used any of the results of catastrophe theory per se. Indeed the reader will observe the ad hoc way in which the imperfection is introduced in the strut and shell models, in the hope that this will lead to a generic potential - as it appears to do when we finally arrive at the quartic local approximations. In the arch we arrive at a local quartic without introducing any such imperfection, and because the local expansion is about a boundary point $(a = 0)$ instead of an interior point in the control plane, catastrophe theory apparently does not yet assure us that this quartic is generic (see Sewell [1], p. 172). However, certain ad hoc imperfections introduced into the arch have been found to induce a change of smaller order in the maximum load, in contrast to the larger order associated with the cusp in the strut and shell models.

It is clear that many areas of classical and recent science offer examples of equilibrium surfaces and bifurcation sets waiting to be reappraised in terms of a full geometrization like that presented here, and to be investigated from the catastrophe theory viewpoint to discover, for example, if their potentials can be significantly altered by a small perturbing term, or instead are 'structurally stable'. The 'dynamic' associated with such problems might vary in character from case to case. As far as elementary catastrophe theory is concerned, any problem characterized by a discretizable variational principle might be examined from the suggested viewpoint.

We close by offering three more normalized potentials generating equilibrium surfaces which the reader might care to plot and relate to

-40-

classical results.   The first concerns a single particle of mass m and

angular momentum p moving under a central force μr^{-n} (given positive

μ and n) at a distance r from the origin.   The effective potential is

$$V(r; n, c) = \frac{r^{1-n}}{1-n} + \frac{c}{2r^2}$$

where r is the behaviour variable $(0 < r < \infty)$, and the mathematical

control variables are n $(0 \leqslant n < \infty)$ and $c \equiv p^2/m\mu$ $(0 < c < \infty)$.   'Equilibria'

are circular orbits.

The second example is an axisymmetric top inclined at an angle θ

to the vertical $(0 < \theta < \pi)$.   This has effective potential

$$V(\theta; c_\phi, c_\psi) = \cos\theta + \frac{1}{2}\left[\frac{c_\phi - c_\psi \cos\theta}{\sin\theta}\right]^2$$

where θ is the behaviour variable, and the mathematical controls are the

normalized momenta c_ϕ, c_ψ $(0 < c_\phi, c_\psi < \infty)$ associated with the Euler

angles ϕ and ψ .   'Equilibria' are conical motions of the axis.   The

above two potentials are derived in standard texts, and also in Sewell [2].

Our last example is a contribution to the theory of phase transitions.

Several authors have observed that boiling or condensation of a gas might

be viewed as catastrophes in the sense of sudden jumps in the value of

the density (= x + 1, say) at suitable temperature t and pressure p .

Thus x is behaviour, and p and t are controls.   The latter are normalized

so that $0 < t < \infty$, $0 < p < \infty$ and so that the so-called liquid/gas 'critical'

point is at x = 0, t = p = 1 .   Restrict attention to the domain -1 < x < 2

containing the liquid/gas point as an interior point. Then it was shown by

Sewell [4] that the van der Waal's model emerges from the generating po-

tential

$$V(x; t, p) = \Phi(x) \Psi(x; t, p)$$

where

$$\Phi(x) = \frac{1}{3}(1 + x)^2 (2 - x) > 0$$

$$\Psi(x; t, p) = \frac{1}{x+1} - 3(x+1) - \frac{8}{3}(t+1) \log\left[\frac{3}{x+1} - 1\right] + \frac{p}{x+1} + \text{constant},$$

in which the datum constant is always chosen to make $\Psi = 0$ when

$$\Phi \frac{\partial \Psi}{\partial x} = 0 .$$

This last equation of thermomechanical equilibrium then implies $\partial V/\partial x = 0$,

and is the cubic

$$x^3 + \frac{x(8t + p)}{3} + \frac{(8t - 2p)}{3} = 0 .$$

This is equivalent to van der Waal's equation, but in a form recognized

by Fowler as the folded equilibrium surface of Thom's cusp catastrophe,

like the local shapes obtained for the above arch, strut and shell models.

Acknowledgement

REFERENCES

Budiansky, B.   [1] Theory of buckling and post-buckling of elastic structures, Advances in Applied Mechanics 14, 1-65, 1974, Academic Press.

Hutchinson, J. W. [1] Plastic buckling, Advances in Applied Mechanics 14, 87-144, 1974, Academic Press.

Koiter, W. T.   [1] Elastic stability and post-buckling behaviour, pp. 257-276 of Nonlinear Problems (edited by R. E. Langer), University of Wisconsin Press, 1963.

Poston, T. and Stewart, I. N.   [1] Taylor Expansions and Catastrophes, Pitman, London, 1976.

Poston, T. and Woodcock, A. E. R.   [1] Zeeman's catastrophe machine, Proc. Camb. Phil. Soc. 74, 217-226, 1973.

Sewell, M. J.   [1] Some mechanical examples of catastrophe theory, Bulletin of the Institute of Mathematics and its Applications 12, 163-172, 1976.

Sewell, M. J.   [2] On the connection between stability and the shape of the equilibrium surface, J. Mech. Phys. Solids 14, 203-230, 1966.

                         [3] A survey of plastic buckling, pp. 85-197 of Stability (edited by H. Leipholz), University of Waterloo, 1972.

                         [4] Elementary catastrophe theory, in Proceedings of the Interdisciplinary Conference on Problem Analysis in Science and Engineering (edited by K. Huseyin), Academic Press, 1976.

Thom, R.   [1] Topological models in biology, Topology 8, 313-336, 1969.

                         [2] Structural Stability and Morphogenesis, W. A. Benjamin Inc., Reading, Mass., 1975.

Zeeman, E. C.   [1] Differential equations for the heartbeat and nerve impulse, Towards a Theoretical Biology (edited by C. H. Waddington) 4, 8-67, 1972.

REPORT DOCUMENTATION PAGE		READ INSTRUCTIONS BEFORE COMPLETING FORM
1. REPORT NUMBER 1714	2. GOVT ACCESSION NO.	3. RECIPIENT'S CATALOG NUMBER Technical
4. TITLE (and Subtitle) SOME GLOBAL EQUILIBRIUM SURFACES		5. TYPE OF REPORT & PERIOD COVERED Summary Report, no specific reporting period
		6. PERFORMING ORG. REPORT NUMBER
7. AUTHOR(s) M. J. Sewell		8. CONTRACT OR GRANT NUMBER(s) DAAG29-75-C-0024
9. PERFORMING ORGANIZATION NAME AND ADDRESS Mathematics Research Center, University of 610 Walnut Street Wisconsin Madison, Wisconsin 53706		10. PROGRAM ELEMENT, PROJECT, TASK AREA & WORK UNIT NUMBERS 3 - Applications of Mathematics
11. CONTROLLING OFFICE NAME AND ADDRESS See Item 18 below.		12. REPORT DATE February 1977
		13. NUMBER OF PAGES 44
14. MONITORING AGENCY NAME & ADDRESS(if different from Controlling Office) 47 p.		15. SECURITY CLASS. (of this report) UNCLASSIFIED
		15a. DECLASSIFICATION/DOWNGRADING SCHEDULE

16. DISTRIBUTION STATEMENT (of this Report)   MRC-TSR-1714

Approved for public release; distribution unlimited.

17. DISTRIBUTION STATEMENT (of the abstract entered in Block 20, if different from Report)

18. SUPPLEMENTARY NOTES

U.S. Army Research Office   Department of Mathematics
P.O. Box 12211   University of Reading
Research Triangle Park   United Kingdom
North Carolina 27709

19. KEY WORDS (Continue on reverse side if necessary and identify by block number)

Bifurcation, Catastrophe, Buckling, Elasticity, Stability, Equilibrium, Structures.

20. ABSTRACT (Continue on reverse side if necessary and identify by block number)

Global equilibrium surfaces in three dimensions are described by elementary functions in closed form for models of loaded arches, struts and shells. They are computed and displayed graphically, in a form which shows their relation with the cusp catastrophe potential.

DD FORM 1473 EDITION OF 1 NOV 65 IS OBSOLETE
1 JAN 73